

1

Supplemental file

2 **Green synthesis and characterization of Ag nanoparticles in phytic acid/ascorbic**
3 **acid/sodium hydroxide system and their application in electrochemical detection**
4 **of H₂O₂**

5 Baolong Niu ^{a, b} **, Hong Wang ^{a, b}, Yanwei Zhang ^{a, b}, Bin Nie ^{a, b}, Huifang Wang ^b, Xiaojie Lian ^{c, d},

6 Wenfeng Li ^{a, b} *

7 ^aCollege of Materials Science and Engineering, Taiyuan University of Technology, Taiyuan
8 030024, PR China;

9 ^bKey Laboratory of Interface Science and Engineering in Advanced Materials, Taiyuan University
10 of Technology, Ministry of Education, Taiyuan 030024, PR China;

11 ^cDepartment of Biomedical Engineering, Research Center for Nano-biomaterials & Regenerative
12 Medicine, College of Biomedical Engineering, Taiyuan University of Technology, Taiyuan 030024,
13 PR China;

14 ^dShanxi Key Laboratory of Material Strength & Structural Impact, Institute of Biomedical
15 Engineering, Taiyuan University of Technology, Taiyuan 030024, PR China.

16 *Corresponding author

17 **Baolong Niu**

18 Address: College of Materials Science and Engineering, Taiyuan University of Technology, Key
19 Laboratory of Interface Science and Engineering in Advanced Materials, Taiyuan 030024, PR China

20 Phone: 0086-351-6111197

21 Fax: 0086-351-6111190

22 E-mail: baolongniutyut@hotmail.com

23 **Wenfeng Li**

24 Address: College of Materials Science and Engineering, Taiyuan University of Technology, Key
25 Laboratory of Interface Science and Engineering in Advanced Materials, Taiyuan 030024, PR China

26 Phone:0086-351-6111197

27 Fax: 0086-351-6111190

28

29 **1. Materials and methods**

30 **1.1. Orthogonal test**

31 The factors and levels of the orthogonal test were shown in Table S1. Since the
 32 orthogonal experiment involved 6 factors and 5 levels, the orthogonal table ($L_{25}(5^6)$) as
 33 shown in Table S2 was designed. Then, the factors and levels were corresponding to
 34 the orthogonal table ($L_{25}(5^6)$) to obtain the experimental program, as shown in Table
 35 S3.

36 Table S1. Factors and levels of orthogonal test.

Factor Level	A	B	C	D	E	F
	Concentration of AgNO ₃ (mM)	PA dosage	AA dosage	The pH of solution A	The pH of solution C	Reaction temperature (°C)
1	7	0.5:1	0.5:1	7	7	25
2	8	1:1	1:1	8	8	40
3	9	2:1	2:1	9	9	50
4	10	3:1	3:1	10	10	60
5	11	4:1	4:1	11	11	70

37 Note: PA and AA dosage were expressed as n(PA):n(AgNO₃) and n(AA):n(AgNO₃), respectively.

38 Table S2. Orthogonal table ($L_{25}(5^6)$).

Test number	Column					
	1	2	3	4	5	6
1	1	1	1	1	1	1
2	1	2	2	2	2	2
3	1	3	3	3	3	3
4	1	4	4	4	4	4
5	1	5	5	5	5	5
6	2	1	2	3	4	5
7	2	2	3	4	5	1
8	2	3	4	5	1	2
9	2	4	5	1	2	3
10	2	5	1	2	3	4
11	3	1	3	5	2	4
12	3	2	4	1	3	5

13	3	3	5	2	4	1
14	3	4	1	3	5	2
15	3	5	2	4	1	3
16	4	1	4	2	5	3
17	4	2	5	3	1	4
18	4	3	1	4	2	5
19	4	4	2	5	3	1
20	4	5	3	1	4	2
21	5	1	5	4	3	2
22	5	2	1	5	4	3
23	5	3	2	1	5	4
24	5	4	3	2	1	5
25	5	5	4	3	2	1

39

Table S3. Testing program.

Test number	Combination of levels	Test condition					Reaction temperature (°C)
		Concentration of AgNO ₃ (mM)	PA dosage	AA dosage	The pH of solution A	The pH of solution C	
1	A ₁ B ₁ C ₁ D ₁ E ₁ F ₁	7	0.5:1	0.5:1	7	7	25
2	A ₁ B ₂ C ₂ D ₂ E ₂ F ₂	7	1:1	1:1	8	8	40
3	A ₁ B ₃ C ₃ D ₃ E ₃ F ₃	7	2:1	2:1	9	9	50
4	A ₁ B ₄ C ₄ D ₄ E ₄ F ₄	7	3:1	3:1	10	10	60
5	A ₁ B ₅ C ₅ D ₅ E ₅ F ₅	7	4:1	4:1	11	11	70
6	A ₂ B ₁ C ₂ D ₃ E ₄ F ₅	8	0.5:1	1:1	9	10	70
7	A ₂ B ₂ C ₃ D ₄ E ₅ F ₁	8	1:1	2:1	10	11	25
8	A ₂ B ₃ C ₄ D ₅ E ₁ F ₂	8	2:1	3:1	11	7	40
9	A ₂ B ₄ C ₅ D ₁ E ₂ F ₃	8	3:1	4:1	7	8	50
10	A ₂ B ₅ C ₁ D ₂ E ₃ F ₄	8	4:1	0.5:1	8	9	60
11	A ₃ B ₁ C ₃ D ₅ E ₂ F ₄	9	0.5:1	2:1	11	8	60
12	A ₃ B ₂ C ₄ D ₁ E ₃ F ₅	9	1:1	3:1	7	9	70
13	A ₃ B ₃ C ₅ D ₂ E ₄ F ₁	9	2:1	4:1	8	10	25
14	A ₃ B ₄ C ₁ D ₃ E ₅ F ₂	9	3:1	0.5:1	9	11	40
15	A ₃ B ₅ C ₂ D ₄ E ₁ F ₃	9	4:1	1:1	10	7	50
16	A ₄ B ₁ C ₄ D ₂ E ₅ F ₃	10	0.5:1	3:1	8	11	50
17	A ₄ B ₂ C ₅ D ₃ E ₁ F ₄	10	1:1	4:1	9	7	60

18	A ₄ B ₃ C ₁ D ₄ E ₂ F ₅	10	2:1	0.5:1	10	8	70
19	A ₄ B ₄ C ₂ D ₅ E ₃ F ₁	10	3:1	1:1	11	9	25
20	A ₄ B ₅ C ₃ D ₁ E ₄ F ₂	10	4:1	2:1	7	10	40
21	A ₅ B ₁ C ₅ D ₄ E ₃ F ₂	11	0.5:1	4:1	10	9	40
22	A ₅ B ₂ C ₁ D ₅ E ₄ F ₃	11	1:1	0.5:1	11	10	50
23	A ₅ B ₃ C ₂ D ₁ E ₅ F ₄	11	2:1	1:1	7	11	60
24	A ₅ B ₄ C ₃ D ₂ E ₁ F ₅	11	3:1	2:1	8	7	70
25	A ₅ B ₅ C ₄ D ₃ E ₂ F ₁	11	4:1	3:1	9	8	25

40 1.2. Stability test of Ag NPs@PA

41 1.2.1. Stability of storage

42 In order to clarify the storage stability of Ag NPs@PA sol at 4 °C, in this
43 experiment, the sols stored at 4 °C for different times (0, 1, 3, 5, and 6 weeks) were
44 tested using UV spectrophotometer. The samples were diluted 20 times for each test,
45 and three parallel experiments were performed and the average value was taken. The
46 relative stability is the ratio of the absorption peak intensity of each test to the
47 absorption peak intensity of the initial storage time.

48 1.2.2. pH stability

49 To verify the stability of Ag NPs@PA under different harsh conditions, some
50 experiments were carried out on the sol under different pH environments ¹. Firstly,
51 deionized water with different pH (6–14) was configured. The samples were then
52 diluted 20-fold with deionized water of different pH, and the mixture was incubated for
53 2 hours at room temperature. Finally, the mixture was transferred to a quartz cuvette for
54 absorbance measurement, and three parallel experiments were performed for each
55 group and the average value was taken. The highest value was defined as 100% relative
56 stability.

57 1.2.3 Stability of temperature

58 In addition to different pH environments, further experiments were carried out at
59 different temperatures ¹. The samples were first diluted 20-fold, and then the dispersions
60 were incubated at different temperatures (4, 25, 30, 60, 70 °C) for 2 h. Finally,
61 absorbance measurements were performed in a quartz cuvette. Similarly, three parallel
62 experiments were performed for each group and the average value was taken. The

63 highest value was defined as 100% relative stability.

64 1.3. Selectivity of electrochemical H₂O₂ sensors

65 The time-current test was used to detect 6 substances including 0.1 mM H₂O₂, 1
66 mM NaCl, 1 mM citric acid (CA), 1 mM urea, 1 mM glucose (Glu) and 1 mM ascorbic
67 acid (AA) using sensors. The test potential was -0.5 V vs SCE.

68 1.4. Anti-interference of electrochemical H₂O₂ sensor

69 Sensors were used to detect the changes of the electrochemical response signal of
70 1 mM H₂O₂ in the presence and absence of 1 mM NaCl, 1 mM citric acid, 1 mM urea,
71 1 mM glucose and 1 mM ascorbic acid.

72 1.5. Repeatability and reproducibility of electrochemical H₂O₂ sensors

73 The same sensor was used to detect 1 mM H₂O₂ for four times, and the
74 electrochemical response signal was compared to verify the repeatability of the sensor.
75 In addition, three electrodes were made by the same method to detect 1 mM H₂O₂, and
76 the relative standard deviation (RSD) was calculated to study the reproducibility of the
77 sensor.

78 1.6. Test of electrochemical H₂O₂ sensor in real samples

79 In order to evaluate the feasibility of the simple electrochemical H₂O₂ sensor in
80 practical application, this sensor was used to detect the electrochemical response signal
81 when 500 μM H₂O₂ was added to real samples such as purified water, tap water and
82 Fenhe water, and the recovery rate of each water sample was studied.

83 2. Results and discussion

84 2.1. Optimization of preparation conditions for Ag NPs@PA

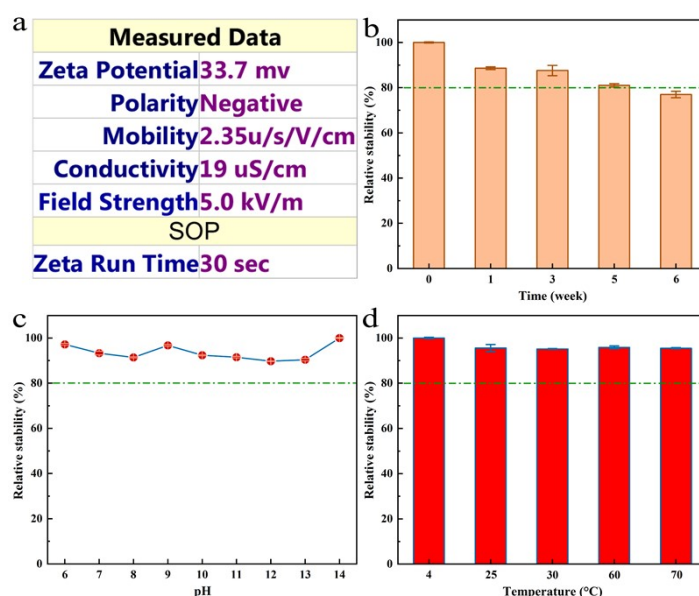
85 Table S4. Analysis of test results.

T-Values	Peak position (nm)						Half-peak width (nm)						Peak intensity (a.u.)					
	A	B	C	D	E	F	A	B	C	D	E	F	A	B	C	D	E	F
T ₁	2056.5	2300	2089.5	2091.5	2056	2106.5	1159.73	1218.33	921.56	1041.59	988.65	1476.37	6.441	8.877	6.596	7.221	8.147	3.675
T ₂	1981	2018	1992.5	2100	2026	2144.5	787.34	973.53	953.68	1258.97	1101.13	1108.69	8.259	8.214	7.445	6.305	7.956	6.471

88 Figure S1. SEM images of Ag NPs@PA at (a) 100000、 (b) 200000 magnification times and their
89 (c) particle size distribution.

90 Figure S1a, b displayed SEM images of Ag NPs@PA at different magnifications.
91 It can be seen from the figure that the morphology of Ag NPs@PA is almost spherical,
92 and the particles are monodisperse, which was the same as the conclusion obtained in
93 TEM. In addition, statistics were also carried out for the nanoparticles in Figure S1b,
94 and the particle size distribution results were shown in Figure S1c. The particle size
95 distribution ranged from 3-17 nm and the average particle size is 9.05 nm, which was
96 consistent with the conclusion of TEM.

97 2.3. Stability of Ag NPs@PA



98
99 Figure S2. (a) ZETA potential of Ag NPs@PA and their stability under different conditions:
100 (b) time, (c) pH, (d) temperature.

101 The stability of sol is closely related to the convenience of storage and further
102 application. It has been reported that nanoparticle sol is stable when its ZETA potential
103 range is beyond ± 20 mV². Figure S2a exhibited that the ZETA potential of the Ag
104 NPs@PA sol is -33.7 mV, indicating that the Ag NPs@PA sol has sufficient stability,
105 which was the result of PA acting as dispersant and stabilizer to play a steric hindrance
106 and the same charge repulsion between particles to avoid agglomeration.

107 In addition, as shown in Figure S2b, the Ag NPs@PA sol was continuously
108 monitored for 6 weeks, and it was found that the relative stability of the sol remained

109 above 80% after 5 weeks, which also indicated that the sol was very stable. This storage
110 stability also depended on the effective coating of Ag NPs by PA and was significantly
111 affected by the antioxidant properties of PA molecules. Its antioxidant ability was
112 derived from the fact that each PA molecule can provide 6 pairs of hydrogen atoms to
113 form a stable structure for the electrons of free radicals, thus replacing Ag NPs as the
114 oxidized molecules.

115 In order to investigate the stability of the sol in practical application, two external
116 environmental factors such as pH and temperature were also arranged to test the Ag
117 NPs@PA sol. As can be seen from Figure S2c, the relative stability of the sol was much
118 higher than 80% in the wide range (pH=6–14) of weak acid, neutral and basic,
119 indicating that the sol has a strong environmental adaptability in terms of pH. This is
120 because PA had a high degree of ionization in the pH range of weak acid, neutral and
121 basic. The strong electrostatic repulsion between the PA coated on the surface of
122 different Ag NPs ensured the stability of Ag NPs@PA. Figure S2d showed the stability
123 test of Ag NPs@PA sol at different temperatures. No matter in low temperature storage
124 environment, room temperature or near high preparation temperature, its relative
125 stability was much higher than 80%, indicating that its stability did not depend on
126 external temperature. Under the low temperature storage environment of 4 °C, the free
127 movement of particles was very inactive, and agglomeration was difficult to occur
128 under the obstruction of PA. With the increase of external temperature, the Brownian
129 motion intensified and the probability of collision between particles increased.
130 However, since Ag NPs were coated by PA, the agglomeration phenomenon was not
131 obvious.

132 **2.4. Selectivity of electrochemical H₂O₂ sensors**

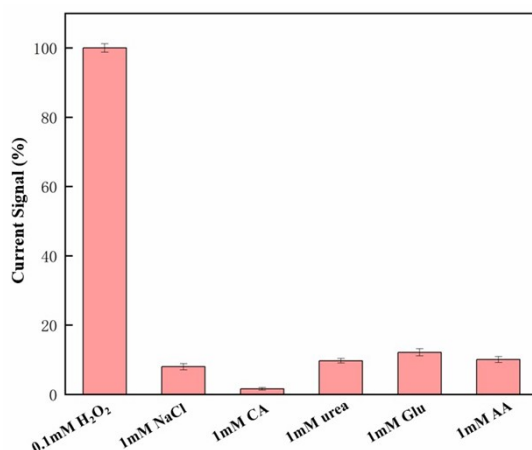


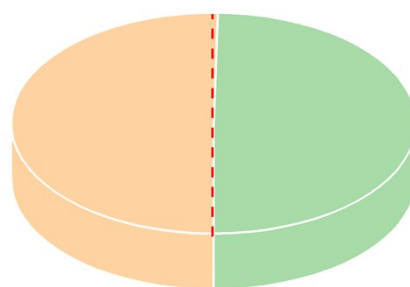
Figure S3. Selectivity of sensor.

133

134

135 To study the selectivity of the electrochemical H₂O₂ sensor, the sensor was used
 136 to detect H₂O₂, NaCl, citric acid, urea, glucose and ascorbic acid, as shown in Figure
 137 S3. It can be found from the response signal in the figure that even though the
 138 concentration of H₂O₂ was only 1/10 of the other interfering substances, its response
 139 signal was still much stronger than NaCl, citric acid, urea, glucose and ascorbic acid,
 140 which was enough to manifest that the sensor has excellent selectivity for the detection
 141 of H₂O₂³.

142 2.5. Anti-interference of electrochemical H₂O₂ sensor



■ 1mM H₂O₂ in the absence of interfering species
■ 1mM H₂O₂ in presence of 1mM interfering species (NaCl, CA, urea, Glu, AA)

143

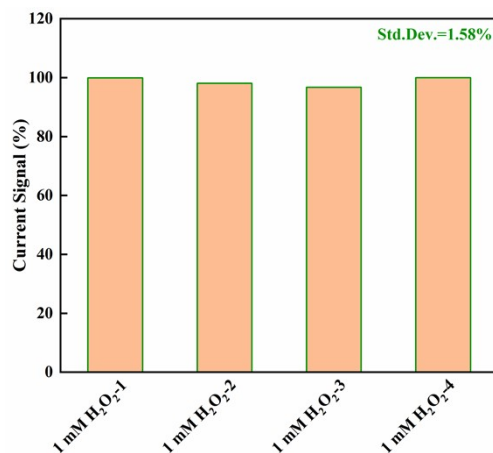
144

Figure S4. Anti-interference of electrochemical H₂O₂ sensor

145 Besides selectivity, the anti-interference ability of the sensor was also investigated.
 146 Figure S4 exhibited the comparison of the response signals of the sensor to detect H₂O₂
 147 with or without interference. It can be seen intuitively that the response signal detected
 148 by the electrochemical H₂O₂ sensor had little change in the presence or absence of
 149 interfering substances, which confirmed that the sensor demonstrated excellent anti-
 150 interference ability for the detection of H₂O₂, which was conducive to its further

151 practical application.

152 2.6. Repeatability and reproducibility of electrochemical H₂O₂ sensors



153

154

Figure S5. Repeatability of the sensor

155 Figure S5 revealed that the electrochemical H₂O₂ sensor possesses good
156 repeatability. The response signal corresponding to the same sensor detecting the same
157 concentration of H₂O₂ kept basically consistent, and the RSD of four tests was only
158 1.58%, indicating that the sensor has good repeatability and can carry out continuous
159 detection, which was of great significance for field detection. Reproducibility is another
160 important sensor performance parameter. Reproducibility is another important sensor
161 performance parameter. The RSD of three electrodes made by the same method to
162 detect the same concentration of H₂O₂ was 3.83%. Therefore, the reproducibility of the
163 electrochemical H₂O₂ sensor was also acceptable.

164 2.7. Application of electrochemical H₂O₂ sensor in real samples

165 Table S5. Recovery rate (%) of H₂O₂ detected by electrochemical H₂O₂ sensor in actual samples.

Sample	H ₂ O ₂ recovered (μL)	Recovery rate (%)	RSD (%)
PBS	500.0	100%	0
Purified water	504.5	100.09%	0.63
Tap water	505.1	101.02%	0.72
Fenhe water	463.8	92.76%	5.31

166 To evaluate the feasibility of the sensor in practical application, the
167 electrochemical H₂O₂ sensor was used to detect the actual samples of purified water,
168 tap water and Fenhe water³. A standard concentration of 500 μM H₂O₂ was added to a

169 given actual water sample, and the recovery of each water sample was researched, as
170 shown in Table S5. It is observed from the table that the recovery rate of the sensor in
171 the three practical samples was relatively ideal, ranging from 92.77% to 101.02%,
172 which can be applied in practical detection.

173

174 **References**

- 175 1. S.-B. He, P. Balasubramanian, Z.-W. Chen, Q. Zhang, Q.-Q. Zhuang, H.-P.
176 Peng, H.-H. Deng, X.-H. Xia and W. Chen, *ACS applied materials & interfaces*,
177 2020, **12**, 14876-14883.
- 178 2. A. M. El Badawy, T. P. Luxton, R. G. Silva, K. G. Scheckel, M. T. Suidan and T.
179 M. Tolaymat, *ENVIRONMENTAL SCIENCE & TECHNOLOGY*, 2010, **44**,
180 1260-1266.
- 181 3. S. Kumar, S. Chaudhary and G. R. Chaudhary, *MATERIALS SCIENCE AND*
182 *ENGINEERING C-MATERIALS FOR BIOLOGICAL APPLICATIONS*, 2020,
183 **114**.
- 184